Study on Local Vibration Control of 100m X-BOW Polar Exploration Cruise Ship

Guo he Jiang , Jia chen Chen , Hao Guo * , Gang Wu , Zhen zhen Liu

Posted Date: 16 April 2024

doi: 10.20944/preprints202404.1001.v1

Keywords: polar exploration cruise; frequency response analysis; modal equivalent mass; tuned mass dampers; mass ratio

 doi:10.20944/preprints202404.1001.v1

Article

Study on Local Vibration Control of 100m X-BOW Polar Exploration Cruise Ship

Guohe Jiang [1], Jiachen Chen [1], Hao Guo [1]*, Gang Wu [1] and Zhenzhen Liu [1]

Merchant Marine College, Shanghai Maritime University, Shanghai 201306, China; guohejiang@shmtu.edu.cn (G.J.); 764139027@qq.com(J.C.); guohao@shmtu.edu.cn (H.G.) ; wugang@shmtu.edu.cn (G.W.); 316650505@qq.com (Z.L.)

* Correspondence: guohao@shmtu.edu.cn

Abstract: A finite element model of 100m X-BOW polar exploration cruise is established. The entire ship frequency response analysis was carried out, comparing the simulated values with the test values, the maximum error is 22%, but only 0.24mm/s difference, the error can be ignored from the perspective of comfort, therefore, the simulation results meet the requirements of engineering accuracy and verify the effectiveness of the model. According to the solution method for global modal equivalent mass, combing the spatial distribution principle of local modal mass, the method for solving the equivalent mass of a single local mode in mixed mode is proposed, the equivalent mass of the local vibration region of 100m X-BOW polar exploration cruise ship is solved by this method, tuned mass dampers mass ratio parameters are calculated using the equivalent mass. According to the analysis, tuned mass dampers has 31dB vibration absorption effect at 13.4Hz when the mass ratio is 0.05, it also has certain control effect at 10Hz and 18.8Hz, the control effect is 3dB and 2dB respectively, the overall control frequency band is flat and robust.

Keywords: polar exploration cruise; frequency response analysis; modal equivalent mass; tuned mass dampers; mass ratio

1. Introduction

The 100m X-BOW polar expedition cruise ship is the first domestic luxury polar expedition cruise ship, this type of ship has the characteristics of multiple equipment, large power, complex hull structure and layout in the engine room, etc. In the design stage, the main frequency of the main excitation force is known, so the main modal frequency of the whole ship and the main excitation frequency can be staggered by optimizing the design of the main hull, so as to prevent the whole ship from resonating. However, the hull structure is intricate and complex, the natural frequency of the whole ship can be adjusted through the early optimization design, it is impossible to make the natural frequency of each local structure avoid the excitation frequency. In the structure of the 100m X-BOW type polar expedition cruise ship, there are large-area local structures, such as the sun platform, viewing platform, etc., whose main natural frequencies are concentrated in the range of 10Hz~18Hz [1] which is easily connected with the propeller and the main engine, causing resonance and affecting passenger comfort, so it is necessary to control local structural vibration. At present, the local vibration of the hull structure is mainly done by optimizing the local structural and changing the structural stiffness to avoid the intrinsic frequency of the main *excitation* [2−5], such as modifying the properties of the beam-column section to strengthen the local structural strength, but these methods only can be implemented during the construction stage. When the whole ship enters the commissioning or sea trial stage, it is no longer possible to make local optimization of the structure. Tuned mass damper (TMD) can effectively control structural vibration, Zong Zhi*xiang* [6] installed multiple dynamic vibration absorbers in the body of urban rail vehicles. According to the principle

 doi:10.20944/preprints202404.1001.v1

of multiple dynamic vibration absorbers and the characteristics of urban rail vehicles including multiple dynamic vibration absorbers is established, and a design method of multiple power absorbers applicable to the body of urban rail vehicles is proposed. Zhang xin*ya* [7] designed and made a similar test model of the rail box girder structure by taking the railway 32m simply supported box girder bridge as a prototype. On the basis of verifying the reliability of the test modal, add the additional control of TMD of the first-order and second-order modal vibration. The vibration response of the measurement point before and after the vibration reduction is obtained by performance a single-point vibration excitation test on the test model, and the vibration reduction performance of the TMD on the box girder bridge is analyzed. Tang Si*cong* [8] analyzed the position-elated terms in the floor-MTMD equation of motion, studied the participation of position in the MTMD vibration reduction control, and proposed an MTMD position optimization method based on the finite element method and the mode shape decomposition method, on this basis, a joint optimization strategy of MTMD parameters and position is formulated. Lian Ji*jiang* [9] studied the feasibility of the application of a new type of eddy-tuned mass damper (EC-TMD) based on offshore wind torch-type infrastructure from tow aspects of theoretical reasoning and engineering application, aiming at the problem pf large vibration detrimental to engineering safety of offshore wind power structures under extreme wind load. The results showed that: under extreme wind load conditions, EC-TMD can effectively reduce the vibration displacement amplitude of tower cylinder top by 21%~33%, which indicates that EC-TMD has engineering application value for vibration reduction of offshore wind torch-type infrastructure. Yang *Ying* [10] used TMD as a vibration control measure to reduce the dynamic response of suspension tunnel tubes under moving loads.

Since 1909, when Frahm first used TMD to control lateral tumbling vibrations in ships, TMD has been used extensively in vibration control of ship structures and equipment.11 Li Bing15 studied the effect of the mass ratio of TMD on the vertical vibration damping effect of steel plants and concluded that the damping effect of the plant with TMD placed at the maximum response is better than that of the plant placed close to the excitation. Chen Ling-shuang16 investigated the effect of PTMD placed in the nacelle on the in-plane vibration response of Barge floating wind turbines and optimised the collision parameters. Zhang Kaidong15 investigated the effect of air-damped TMDs formed by replacing the oil damping in conventional tuned mass dampers with air damping on the vibration control of simply supported girder bridges under pedestrian loads. Zhiwei Su15 proposes a tuned mass damper with negative stiffness using TMD applied to the vibration control of propulsion shaft system, and gives a theoretical and design approach. The control effect of a tuned mass damper with negative stiffness was compared with that of a conventional tuned mass damper and it was found that the control effect of a tuned mass damper with negative stiffness was 10dB better than that of a conventional tuned mass damper. Mohammad Reza Ghasemi16 proposes a TMD using shape memory metals as dampers ,a theoretical design method is given in the paper, and it is used for wave-induced vibrations of jack-up marine platforms, at the same time, four calculation conditions were designed: 2-year regression period, 5-year regression period, 10-year regression period and 100-year regression period. Based on the calculation results of the four conditions, it can be seen that the average reduction of vibration displacement of the platform reaches 43%. Jiang-hai Wu17 applied TMD to pipeline vibration control. Since the control band of a single TMD is narrow, multiple TMDs were installed on the pipeline in order to improve the control bandwidth, which was modelled and simulated using finite elements and compared experimentally, the method effectively improve the control bandwidth of TMDs. At present, TMD is mainly used for the overall vibration mode control, and there are few studies on the local vibration mode control. When the local vibration of hull structure occurs, it is generally the coupling of multiple local modes, and it is difficult to directly judge the participation degree of each local mode.

When the 100m X-BOW polar expedition cruise was in the commissioning or sea trial phase, tests revealed local structural vibrations at the sun deck on deck 7, but it was not possible to optimize the local structural adjustments at this time, so this paper proposes the use of a tuned mass damper (TMD) to control local structural vibration, TMD can be subsequently installed without extensive modification to the hull structure. In this paper, a finite element model of a 100m X-BOW type polar

 doi:10.20944/preprints202404.1001.v1

expedition cruise ship is established, through local modal analysis, the local resonance frequency of the sun deck is determined to be 13.4Hz, which is extremely close to the propeller excitation frequency of 12.5Hz, so 13.4Hz is determined as the control target frequency. Ti-o address the problem that it is difficult to judge the degree of participation of a single local mode when local vibration occurs in the hull structure, this paper proposes a local mode equivalent mass identification method based on the intrinsic mode method, which combines the spatial distribution of the mode masses in the mixed mode, identifies the single local mode in the mixed mode and calculated the equivalent mass of the local mode, and solves for the optimal TMD parameters suitable for the local mode based on the equivalent mass of the local mode. To analyze the optimum mass ratio, the mass ratio was set to 0.005, 0.01,0.02,0.05,0.1 and 0.2, and the frequency response was calculated for each of these mass ratios. The analysis shows that at a mass ratio of 0.05, the tuned mass damper has a 31dB absorption effect at 13.4Hz, and also has some control over the amplitude response at 10Hz and 18.8Hz, 3dB and 2dB respectively, with a flatter overall control band and better robustness.

2. Method

2.1. *Local Mode Equivalent Mass Identification Method Based on Natural Mode Method*

Commented [M1]: We revised heading numbers, please confirm.

2.1.1. Optimal Parameter Design of TMD based on Fixed Point Theory

The mechanical model of TMD is shown in Figure 1, which is mainly composed of mass element, elastic elements and damping elements. According to *literature* [18], it is vibration suppression mechanism is as follows: by adjusting the natural frequency if the tuned mass damper to make it consistent with the excitation main frequency, the vibration energy of the main structure is transferred to the mass block, and the TMD gradually absorbs the vibration energy, while the vibration of the main structure is gradually reduced, which can be reduced to zero from the theoretical point of view.

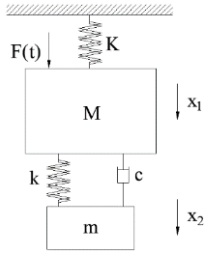

Figure 1. The mechanical model of TMD.

If the displacement of the main systems is, and the mass displacement of the dynamic vibration absorber is, then the equation of motion can be expresses as

$$\begin{cases} M\ddot{x}+c\dot{x}+(K+k)x_1-c\dot{x}_2-kx_2=f=F\sin\omega t \\ m\ddot{x}_2-c\dot{x}_1-kx_1+c\dot{x}_2+kx_2=0 \end{cases} \quad (1)$$

Assuming that f=F$e^{i\omega t}$, $x_1=\overline{X_1}e^{j\omega t}$, x_2=$\overline{X_2}e^{j\omega t}$. Here $\overline{X_1}$ and $\overline{X_2}$ are the complex amplitude of x_1 and x_2 respectively. The solution of Equation (1) can be expressed as

$$\frac{X_1}{X_{st}}(\omega)=\sqrt{\frac{(\gamma^2-\lambda^2)^2+(2\zeta\lambda)^2}{\left[(1-\lambda^2)(\gamma^2-\lambda^2)-\mu\gamma^2\lambda^2\right]^2+\left[1-(1+\mu)\lambda^2\right]^2(2\zeta\lambda)^2}} \quad (2)$$

$$\frac{X_2}{X_{st}}(\omega)=\sqrt{\frac{(\gamma^2)^2+(2\zeta\lambda)^2}{\left[(1-\lambda^2)(\gamma^2-\lambda^2)-\mu\gamma^2\lambda^2\right]^2+\left[1-(1+\mu)\lambda^2\right]^2(2\zeta\lambda)^2}} \quad (3)$$

 doi:10.20944/preprints202404.1001.v1

Where $\Omega_n = \sqrt{\frac{K}{M}}$ represents the natural angular frequency of the main vibration system, $\omega_n = \sqrt{\frac{k}{m}}$ represents the natural angular frequency of TMD, $X_{st} = \frac{F}{K}$ represents the static deformation of the main vibration system, $\mu = \frac{m}{M}$ represents the mass ratio, $\zeta = \frac{c}{2m\Omega_n}$ represents the damping ratio, $\lambda = \frac{\omega}{\Omega_n}$ represents the ratio of the excitation frequency to the natural frequency of the main structure, $\gamma = \frac{\omega_n}{\Omega_n}$ represents the ratio of the TMD natural frequency to the natural frequency of the main structure.

According to *literature* [19], the optimal homology conditional of TMD is

$$\gamma = \frac{\omega_n}{\Omega_n} = \frac{1}{1+\mu} \tag{4}$$

The optimal damping ratio of TMD is

$$\zeta_{opt} = \sqrt{\frac{3\mu}{8(1+\mu)^3}} \tag{5}$$

According to Equation (4) and Equation (5), the mass ratio is crucial for solving the optimal parameters.

2.2. *Local Mode Equivalent Mass Solution Method*

A discontinuous discrete multi-degree of freedom system is established, as shown in Figure 2.

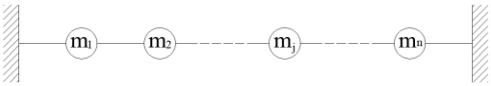

Figure 2. Schematic diagram of a discontinuous multi DOF system.

After decoupling the multi-DOF-system, let the mode mass of the i-th mode be M_i and the vibration velocity be v_i, then the kinetic energy of the mode be

$$T_i = \frac{1}{2} M_i v_i^2 \tag{6}$$

The kinetic energy of the mode i -th is a constant value, but the values of the mode mass M_i and vibration velocity v_i are not unique, and are related to the scaling factor of the mode shape vector, assuming the shape vector of i-th mode be

$$X_i = \{x_{1i}, x_{2i}, \cdots, x_{ni}\}^T \tag{7}$$

In this mode, the vibration velocity of each point is proportional to the mode shape, that

$$V_i = \{\rho x_{1i}, \rho x_{2i}, \cdots, \rho x_{ni}\}^T = \rho\{x_{1i}, x_{2i}, \cdots, x_{ni}\}^T (m/s) \tag{8}$$

Then the total kinetic energy of the system in this mode can be expressed as:

$$T_i = \frac{1}{2}\rho^2\left(m_1 {x_{1i}}^2 + m_2 {x_{2i}}^2 + \cdots + m_n {x_{ni}}^2\right) \tag{9}$$

Take the mode amplitude of the j-th particle is taken as the scaling factor, that

$$T_i = \frac{1}{2}\left(m_1\left(\frac{x_{1i}}{x_{ji}}\right)^2 + m_2\left(\frac{x_{2i}}{x_{ji}}\right)^2 + \cdots + m_j + \cdots + m_n\left(\frac{x_{ni}}{x_{ji}}\right)^2\right)(\rho x_{ji})^2$$
$$= \frac{1}{2} M_{i-j} (\rho x_{ji})^2 \tag{10}$$

This equation is compared with (9)，it can be known that M_{i-j} is the overall modal mass of the i-th mode with x_j as the scaling factor, and point j is the control target point of the i-th mode, M_{i-j}

 doi:10.20944/preprints202404.1001.v1

can be used as the structural reference quality when TMD controls i-th mode, and $m_a\left(\frac{x_{ai}}{x_{ji}}\right)^2$ is the mass distribution of modal M_{i-j} at each point in space, also called the contribution of m_a to the overall modal mass M_{i-j}.

When the k-th mode of the multi-DOF system is assumed to be the local mode, two local modes simultaneously occur, as shown in Figure3, only $m_{j-2}, m_{j-1}, m_j, m_{j+1}, m_{j+2}$ and m_{l-1}, m_l, m_{l+1} vibrate locally.

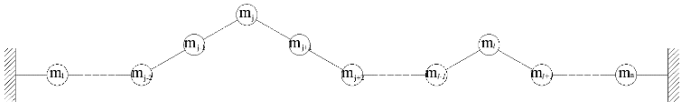

Figure 3. Local modal diagram of multi DOF system.

So, the total kinetic energy is

$$\begin{aligned} T_k &= \frac{1}{2}M_{k-j}(\rho x_j)^2 \\ &= \frac{1}{2}\left(m_{j-2}\left(\frac{x_{(j-2)k}}{x_{jk}}\right)^2 + m_{j-1}\left(\frac{x_{(j-1)k}}{x_{jk}}\right)^2 + m_j + m_{j+1}\left(\frac{x_{(j+1)k}}{x_{jk}}\right)^2 + m_{j+2}\left(\frac{x_{(j+2)k}}{x_{jk}}\right)^2 + \right. \\ &\left. m_{l-1}\left(\frac{x_{(l-1)k}}{x_{jk}}\right)^2 + m_l\left(\frac{x_{lk}}{x_{jk}}\right)^2 + m_{l+1}\left(\frac{x_{(l+1)k}}{x_{jk}}\right)^2\right)(\rho x_{jk})^2 \end{aligned} \tag{11}$$

Assuming

$$M_{local1,k-j} = m_{j-2}\left(\frac{x_{(j-2)k}}{x_{jk}}\right)^2 + m_{j-1}\left(\frac{x_{(j-1)k}}{x_{jk}}\right)^2 + m_j + m_{j+1}\left(\frac{x_{(j+1)k}}{x_{jk}}\right)^2 + m_{j+2}\left(\frac{x_{(j+2)k}}{x_{jk}}\right)^2 \tag{12}$$

$$M_{local2,k-j} = m_{l-1}\left(\frac{x_{(l-1)k}}{x_{jk}}\right)^2 + m_l\left(\frac{x_{lk}}{x_{jk}}\right)^2 + m_{l+1}\left(\frac{x_{(l+1)k}}{x_{jk}}\right)^2 \tag{13}$$

Then

$$T_k = \frac{1}{2}\left(M_{local1,k-j} + M_{local2,k-j}\right)(\rho x_{jk})^2 \tag{14}$$

2.3. *Conversion Method of Concentration Quality Matrix*

By the finite element method, the internal displacement of the cell is generally expressed by interpolation, so that the displacement of each node of the cell is $\{\delta\}^e$, then the internal displacement of the cell is

$$\{u\} = [N]\{\delta\}^e \tag{15}$$

Where $[N]$ is the shape function matrix, the in-cell acceleration is

$$\{\ddot{u}\} = [N]\{\ddot{\delta}\}^e \tag{16}$$

Where $\{\ddot{\delta}\}^e$ is the acceleration matrix of the cell nodes. Using the inertial force $\{\ddot{\delta}\}^e$ in the cell as a volume-distributed load and distributing it to the nodes of the cell according to the distribution principle, we get

$$\{Q\}_\rho^e = -\int [N]^T \rho\{\ddot{u}\}dv \tag{17}$$

Substituting equation (15) into equation (16) gives

Preprints.org (www.preprints.org) | NOT PEER-REVIEWED | Posted: 16 April 2024 doi:10.20944/preprints202404.1001.v1

$$\{Q\}_{\rho}^{e} = -\int [N]^{T} \rho [N] \{\ddot{\delta}\}^{e} dV$$

$$= -\int [N]^{T} \rho [N] dV \{\ddot{\delta}\}^{e} = -[M]^{e} \{\ddot{\delta}\}^{e} \quad (18)$$

Where $[M]^e$ is a consistent mass matrix which is not diagonal, there is some inertial coupling between cells. The consistent mass matrix can be equated to a diagonal matrix, and the equivalent matrix is the concentrated mass matrix.

Let the total kinetic energy of the structure be T, and the total kinetic energy of the sum of the kinetic energies of the cells, that

$$T = \sum T^{e} \quad (19)$$

The kinetic energy of the unit is

$$T^{e} = \frac{1}{2}\int_{V^e} \{\dot{u}\}^{T} \rho \{\dot{u}\} dV = \frac{1}{2}\int_{V^e} \left([N]\{\dot{\delta}\}^{e}\right)^{T} \rho [N] \{\dot{\delta}\}^{e} dV$$

$$= \frac{1}{2}\{\dot{\delta}^{e}\}^{T} \int_{V^e} [N]^{T} \rho [N] dV \{\dot{\delta}\}^{e} = \frac{1}{2}\{\dot{\delta}^{e}\}^{T} [M]^{e} \{\dot{\delta}\}^{e} \quad (19)$$

When the overall mass is equally distributed among all cells, the kinetic energy of each cell is

$$T^{e} = \sum_{k=1}^{n} \frac{1}{2} m_k \dot{\delta}_k^2 \quad (20)$$

Where m_k is the nodal mass corresponding to the displacement component of node k, and n is the number of cell degrees of freedom, at which point the cell mass matrix is diagonal, that

$$[M]^{e} = \begin{bmatrix} m_1 & 0 & 0 & \cdots & 0 \\ 0 & m_2 & 0 & \cdots & 0 \\ 0 & 0 & m_3 & \cdots & 0 \\ \vdots & \vdots & \vdots & \ddots & \vdots \\ 0 & 0 & 0 & \cdots & m_n \end{bmatrix} \quad (21)$$

For thin beam and thin plate and shell units, the kinetic energy of rotation of the nodes can be neglected when using the concentrated mass matrix to represent the structural mass. Assume two-node straight beam cell, i and j being the two nodes, and M being the mass of the cell. However, when the unit masses are equally distributed by the two nodes, the nodal displacements can be expressed as:

$$\{\delta\}^{e} = \begin{bmatrix} \omega_i & \theta_i & \omega_j & \theta_j \end{bmatrix} \quad (22)$$

The the kinetic energy is

$$T^{e} = \frac{1}{2}\frac{M}{2}\dot{\omega}_i^2 + \frac{1}{2}\frac{M}{2}\dot{\omega}_j^2 \quad (23)$$

The concentration mass matrix is

$$[M]^{e} = \begin{bmatrix} \frac{M}{2} & 0 & 0 & 0 \\ 0 & 0 & 0 & 0 \\ 0 & 0 & \frac{M}{2} & 0 \\ 0 & 0 & 0 & 0 \end{bmatrix} \quad (24)$$

3. Finite Element Analysis of 100m X-Bow Local Vibration

3.1.1100. m X-Bow Local Vibration Test

In order to analyze the mode of polar expedition cruise, a finite element model is established. The total length of the model is 104m, the ship's width is 18m, and the waterline height is 5.1m, and

 doi:10.20944/preprints202404.1001.v1

the weight of the ship is 4,265 tons. A centralized mass point simulation device is used, with a coupling between the centralized mass point and the deck picking, and an increase in material density is used to simulated the distribution of additional mass. The added mass and the center of gravity of the model strictly follow the report of weight and center of gravity, as shown in Figure4. The mesh size is mainly 400×400mm, the plate structure is quad 4 element and tria3 element, the beam structure is bar2 element, and the damping factor of the structure is 2% [1]. The 100m X-BOW Polar Expedition Cruiser has twin propellers and twin rudders with a 3100mm oar diameter and 80% rated working speed of 192RPM, the main engine parameters are shown in Table1. According to *literature* [20], the main excitation forces of the ship are main engine excitation and propeller pulsation excitation, and the excitation spectrum is shown in Figure5.

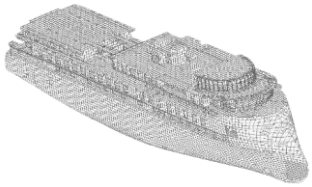

Figure 4. Finite element model of 100m X-BOW polar adventure ship.

Table 1. Host Parameters.

Modal	6L20	8L20
Rated power	1200kW	1600kW
Rated speed	1000RPM	1000RPM
Weight	9.3t	11t
Number	2	2

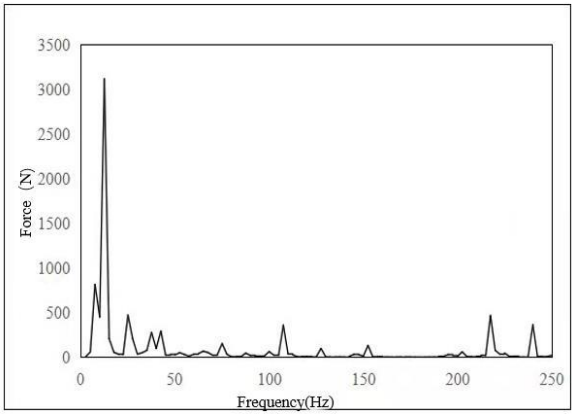

a) Propeller pulsating excitation

 doi:10.20944/preprints202404.1001.v1

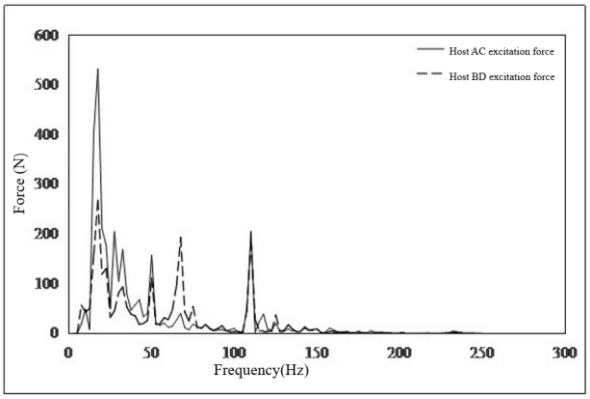

b) Host excitation force

Figure 5. Main excitation spectrum diagram.

The excitation in Figure 5 was loaded into the finite element model to obtain the vibration velocity of each cabin. Several typical regions were selected to compare the vibration response spectrum curve of the central node in these regions with the last value. The comparison curve is shown in Figure 6. It can be seen from the figure that the dominant frequency position of the simulation curve and the test curve can correspond well, and the trend of the curve is basically the same. The effective value pair of vibration velocity is shown in Table 1. The area with the largest error is the sunshine deck on the seventh deck, which is 22% but the difference is only 0.24mm/s. From the perspective of comfort, this error can be ignored, so the simulation results meet the engineering accuracy requirements. It shows that the 100m X-Bow polar cruise ship modal can reflect the actual vibration characteristics of the hull. The reasons for this error mainly come from two aspects: 1） Dressing, outfitting and interior components are omitted in the finite element modal, such as floating bottom plate and interior partition in the four-deck and passenger compartment, which affect the admittance of the transfer path to a certain extent; 2)In the actual measurement, the cruise ship is also affected by the excitation of wind and waves, pumps, steering engines and fans. For example, the second deck-laundry room is affected by the air compressor in the adjacent cabin, so the error is relatively large compared with other areas.

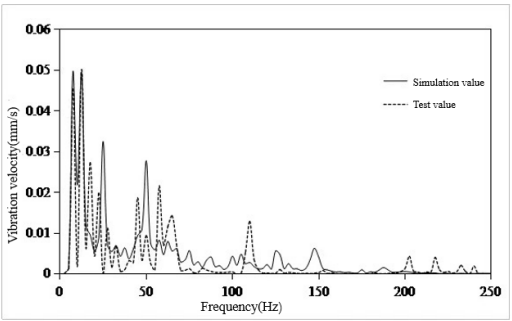

a) Second deck-laundry room

 doi:10.20944/preprints202404.1001.v1

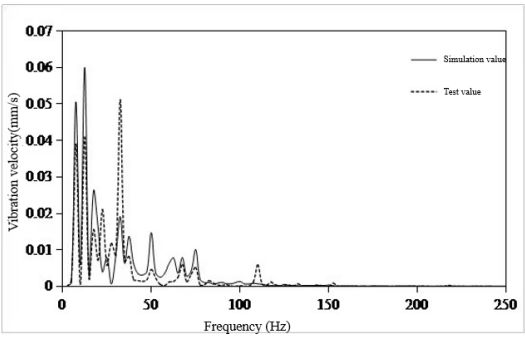

b) Third deck-passenger compartment

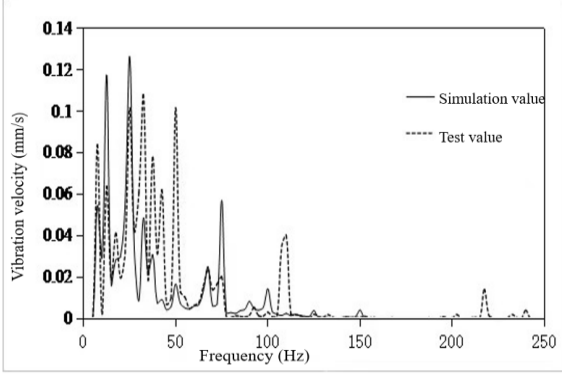

c) Fourth deck-passenger compartment

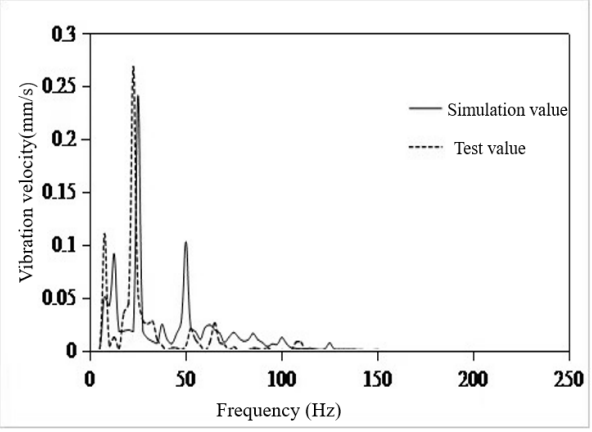

d) Fifth deck-dining room

 doi:10.20944/preprints202404.1001.v1

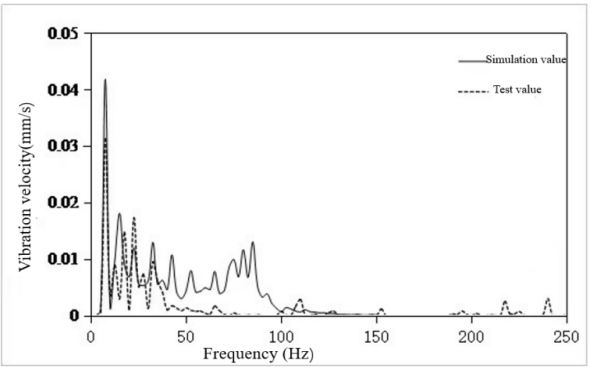

e) sixth deck-passenger compartment

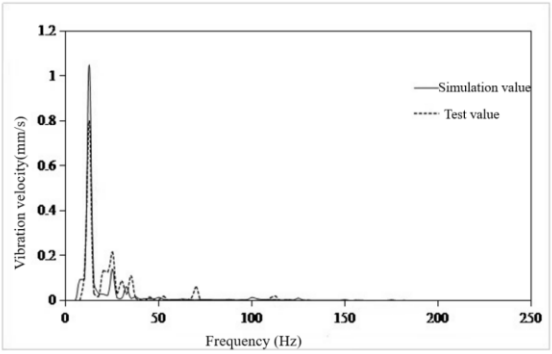

f) Seventh deck-the sun deck

Figure 6. Comparison between simulation value and test value of vibration response.

Table 2. Comparison of vibration response simulation value and test value effective value.

Deck	Area	Test value(mm/s)	Simulation value	Error
DECK7	The sun deck	1.07	0.83	22.43%
DECK6	Passenger compartment	0.046	0.04	13.04%
DECK5	The restaurant	0.31	0.3	3.23%
DECK4	Passenger compartment	0.22	0.18	18.18%
DECK3	Passenger compartment	0.11	0.094	14.55%
DECK2	Laundry room	0.09	0.08	11.11%

 doi:10.20944/preprints202404.1001.v1

3.2. *Local Vibration Control Analysis of TMD*

In order to carry out TMD control on the local vibration of the 100m polar expedition cruise ship, the main frequency of the excitation source should be determined first, and the frequency search range should be determined according to the main frequency of the excitation source, which is generally ±15% of the main frequency of the excitation source. The local modes of the 100m polar expedition cruise ship should be searched in the frequency search range, and the local modes to be controlled should be selected. The modal amplitude and modal mass of the local structure were extracted by Nastran, and the equivalent mass of the local mode was calculated according to Equation (14). Using the equivalent mass, the optimal frequency ratio of TMD was obtained from Equation (4), and the optimal damping ratio of TMD was obtained from Equation (5). The vibration reduction effect of TMD was analyzed by finite element method.

The excitation frequency of 100m X-Bow polar expedition cruise is mainly as follows: the frequency of the propeller excitation blade is 12.5Hz, and the frequency search range is 11.25Hz-13.75Hz. In this range, the modal analysis of the whole ship mode is carried out. After analysis, it is found that at 13.4Hz, there are obvious local modes at the stern of the seventh deck, as shown in Figure 7. It can be seen from Table 2 that the measured value of vibration velocity is 1.07mm/s, which is the highest value among all the measured points in Table 2. Therefore, the local structure in the mode of 13.4Hz is easily induced by the blade of frequency excitation of the propeller to induce resonance effect.

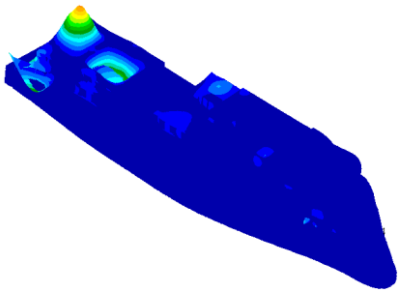

a) Global map of local modes

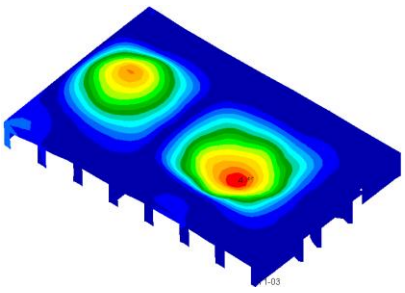

b) Enlarged view of local mode

Figure 7. Local modes of the seventh sun deck.

Because this mode shape is coupled with other local mode shapes, the equivalent mode mass of this local mode shape cannot be calculated by the whole modal. Therefore, it is necessary to extract the centralized mass matrix and modal deformation of each node in the mode shape, and use Equation (14) to calculate the equivalent mass of the local mode. It can be seen from the test that vertical vibration is the main factor affecting the comfort level. So, the vertical vibration mode analysis is given priority to.

 doi:10.20944/preprints202404.1001.v1

There are a total of 1018 nodes in this local structure, and Matlab program is used to extract the centralized mass matrix and modal deformation matrix of nodes, as shown in Equation (25) and (26).

$$M=\begin{bmatrix}0.011 & & & & & & & & & \\ & 0.0288 & & & & & & & & \\ & & 0.0348 & & & & 0 & & & \\ & & & 0.0374 & & & & & & \\ & & & & 0.0341 & & & & & \\ & & & & & 0.037 & & & & \\ & & 0 & & & & 0.0641 & & & \\ & & & & & & & 0.0323 & & \\ & & & & & & & & \ddots & \\ & & & & & & & & & 0.0059\end{bmatrix}_{(1018\times1018)} \quad (25)$$

$$D=\begin{bmatrix}-0.0637 & & & & & & & & & \\ & -0.0342 & & & & & & & & \\ & & -0.053 & & & & 0 & & & \\ & & & -0.0279 & & & & & & \\ & & & & 0.0604 & & & & & \\ & & & & & 0.0888 & & & & \\ & & 0 & & & & 0.1127 & & & \\ & & & & & & & 0.1397 & & \\ & & & & & & & & \ddots & \\ & & & & & & & & & -0.0458\end{bmatrix}_{(1018\times1018)} \quad (26)$$

By substituting the diagonal elements in Equation (25) and (26) into Equation (14), Equation (27) can be obtained, that:

$$T=\sum_{i=1}^{1018}M_i\left(\frac{D_i}{D_{\max}}\right)^2 \quad (27)$$

Where D_{max} is the maximum value in the modal deformation.

The equivalent mass of the local structure at 13.4Hz is 3.46 tons. In order to analyze the influence of mass ratio on vibration absorption effect, the mass ratio was set as 0.005,0.01,0.02,0.05,0.1 and 0.2.and the mass ratio was substituted into Equation (4) and (5) to obtain the frequency ratio γ and the optimal damping ratio ξ_{opt} under optimal homology condition, through calculation, the parameters are shown in Table 3. Since the mode is the second-order mode with double peaks, two TMD need to be set, and one TMD is loaded on each peak, the total mass and total stiffness of the two TMD are corresponding to the parameters in Table 3, and the TMD loading diagram is shown in Figures 3–5, which is connected with node 2566 and node 41807 respectively. The point element is used to represent the mass element, the Beam element is used to represent the spring element, and the spring and damping properties are given.

Table 3. Parameters of TMD.

Quality ration	The total quality of TMD(T)	The total rigidity of TMD(N/m)	γ	ξ_{opt}
0.50%	0.017	122.8	0.995	0.043
1%	0.035	243	0.99	0.06
2%	0.069	476.7	0.98	0.085
5%	0.173	1124.7	0.95	0.13
10%	0.346	2049.5	0.91	0.185
20%	0.69	3444.3	0.83	0.25

 doi:10.20944/preprints202404.1001.v1

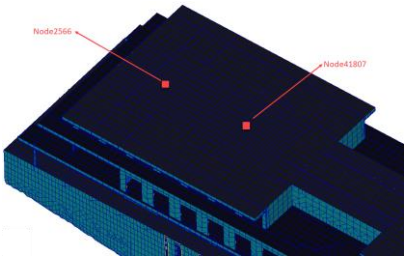

Figure 8. Location of TMD.

Commented [M2]: Please cite the figure in the text and ensure that the first citation of each figure appears in numerical order.

The frequency response analysis of the unit force of the whole ship is carried out, and the frequency response curve under each working condition at node 2566 is taken, as shown in Figure 9. Form Figure 9a, the local structure has three orders of modes within 20Hz, the first order is 10Hz, the second order is 13.4Hz, and the third order is 18.8Hz, where the second order mode is the main control target. After loading the TMD, the control effect of the response at 13.4Hz is more obvious, but some working conditions have a certain amplification effect on the response at 10Hz and 18.8Hz. The response of the frequency band from 12Hz to 15Hz is amplified as shown in Fig.9b, which shows that when the mass ratio is small, as the mass ratio increase, the vibration absorption effect of the TMD becomes obvious and the response curve is flat.

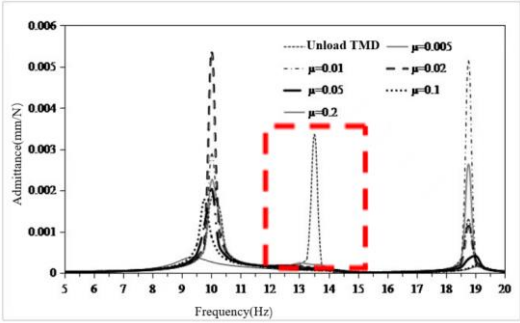

a) Frequency response curve of node 2566 under various working conditions

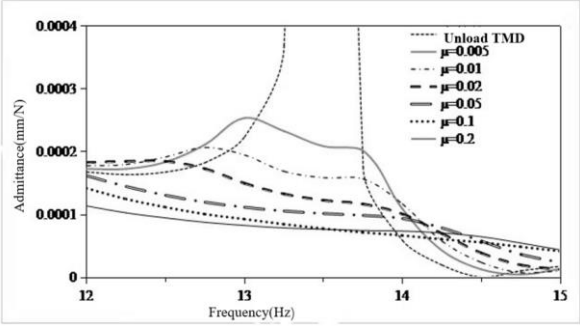

b) Zoom in at 12Hz to 15Hz

Figure 9. Frequency response at node 2566 after TMD installation.

Commented [M3]: E moved figure 9 after first citation, please confirm.

 doi:10.20944/preprints202404.1001.v1

In order to obtain the most suitable TMD scheme for this structure from Table 3, the control effect of TMD response at 13.4Hz and the amplification effect at 10Hz and 18.8Hz need to be comprehensively evaluated. The control effect can be evaluated through Equation (28), that

$$\Delta L = 20\lg(X_0 / X_1) \qquad (28)$$

Where X_0 is the vibration amplitude at 13.4Hz when TMD is not installed, X_1 is the vibration amplitude at 13.4Hz after TMD is installed, and ΔL is the control effect. When evaluation the control effect of TMD, the large ΔL is, the better, when evaluation the magnification effect of TMD, the smaller ΔL is, the better.

The control effect of each working condition is evaluated, Figure10 shows the control effect at 13.4Hz. It can be seen from Figure 10 that when μ is in the range of 0.005~0.05, the control effect of TMD is significantly improved from 24dB to 31dB. When μ>0.05, the control effect of TMD does not increase significantly, increasing from 31dB to 33dB. When μ=0.1 and μ=0.2, the control effect is basically no difference, therefore, it is recommended that the quality ratio μ≤0.05. Figures 11 and 12 show the control effect at 10Hz and 18.8Hz, respectively. As can be seen from the figure, at these two frequency points, there is always a mass ratio μ′, which makes ΔL reach the peak, when $\mu = \mu'$ TMD has the worst control effect at 10Hz and 18.8Hz, and even has the amplification effect. At 10Hz, $\mu' = 0.01$, the TMD amplitude effect is 4dB, at 18.8Hz, $\mu' = 0.02$, the TMD amplification effect is 3.7dB, and when $\mu \neq \mu'$, TMD has a certain control effect on the amplitude at 10Hz and 18.8Hz.

To sum up, for this local structure, it is recommended to take $\mu = 0.05$, at this time, the control effect at 10Hz is 31dB, which has the highest control cost performance, at the same time, the amplitude response at 10Hz and 18.8Hz also has a certain control effect, which is 3dB and 2dB respectively.

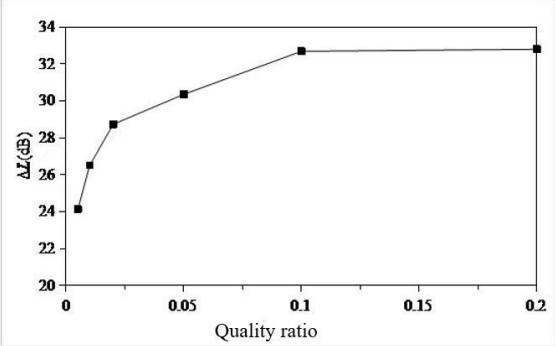

Figure 10. Control effect at 13.4Hz.

 doi:10.20944/preprints202404.1001.v1

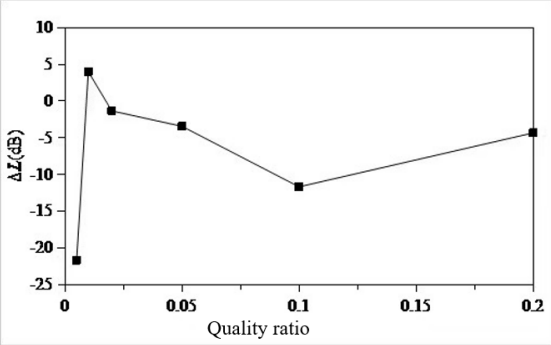

Figure 11. Control effect at 10Hz.

Commented [M4]: Please cite the figure in the text and ensure that the first citation of each figure appears in numerical order.

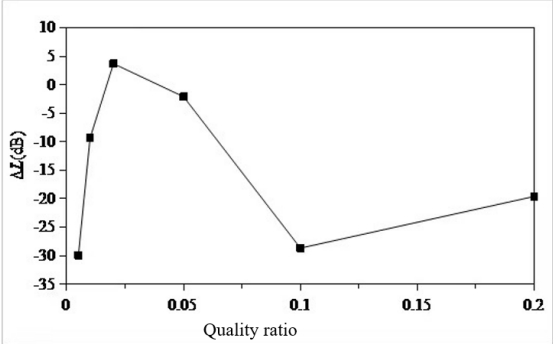

Figure 12. Control effect at 18.8Hz.

Commented [M5]: Please cite the figure in the text and ensure that the first citation of each figure appears in numerical order.

After TMD parameters are selected, TMD is installed on the model loaded with excitation source, and the vibration velocity response is calculated. The vibration velocity response before and after TMD installation is compared, as shown in Figure 13. It can be seen from Figure 13 that after TMD installation, the response near 13.4Hz decreases from 0.8mm/s to 0.13mm/s. It shows that TMD has good control effect.

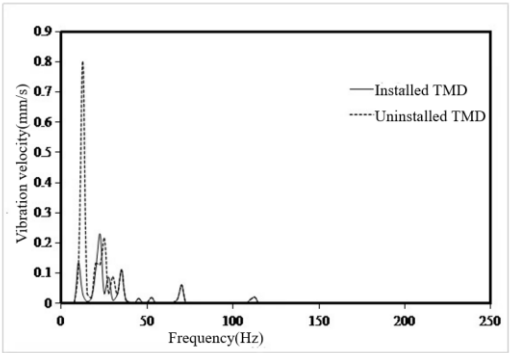

Figure 13. Comparison of responses before and after TMD control on the seventh sun deck.

Commented [M6]: Figure 13 is moved after first citation, please confirm.

 doi:10.20944/preprints202404.1001.v1

4. Conclusions

1. According to the global mode equivalent mass solution method and the spatial destruction principle of local mode mass, a solution method of single local mode equivalent mass in mixed modes is proposed, and the single local mode equivalent mass of the seventh layer sun deck in 100m X-Bow polar exploration cruise ship is solved by using this method.
2. The finite element model of 100m X-Bow polar cruise ship was established to predict the structural vibration response. Six typical cabins were selected, and the simulation value of vibration response of these six cabins was compared with the test value. The frequency response curve trend was basically the same, and the effective value error of vibration response was within 22%, but the difference was only 0.24mm/s. The error can be ignored, so the simulation results meet the engineering accuracy requirements, and verify the effectiveness of the model, which can be used for vibration control analysis.
3. The main excitation frequency was determined to be 12.5Hz. Based on this frequency, the local mode search of the whole ship model was carried out, and the search range was 11.25Hz-13.75Hz. Finally, the natural frequency of the seventh layer sun deck was determined to be in the range of 11.25Hz-13.75Hz, which was consistent with the propeller excitation blade frequency, and there was resonance risk. This area is the area with the largest test response, and the vibration speed is 1.07mm/s. It is necessary to control the vibration in this area.
4. Using the local mode equivalent mass solution method, the local equivalent mass of the seventh layer of the sun deck is solved. The mass ratio μ is set as 0.005,0.01,0.02,0.05,0.1,0.2. According to the six mass ratios, the six optimal parameters of TMD are determined. The optimal mass ratio of TMD in this region is determined to be 0.05. When the mass ratio of TMD is 0.05, the TMD has the vibration absorption effect of 31dB at 13.4Hz, and the amplitude response at 10Hz and 18.8Hz also has certain control effect, which are 3dB and 2dB respectively. The overall control frequency band is flat and the robustness is good. After TMD was installed on the model loaded with excitation source, the response around 13.4Hz decreased from 0.8mm/s to 0.13mm/, indicating that TMD has a good control effect.

Funding: The authors disclosed receipt of the following financial support for the research, authorship, and/or publication of this article: this work was supported by the Science & Technology Commission of Shanghai Municipality and Shanghai Engineering Research Center of Ship Intelligent Maintenance and Energy Efficiency (Grant No. 20DZ2252300), and shanghai Maritime University.

Conflicts of Interest: The author declares that there is no conflict of interest regarding the publication of this paper.

Reference

1. DNVGL.Vibration analysis report [R].U11058_101-012,2018.
2. Shuai Bing. Local Vibration Analysis of a Container Ship Engine-room and Superstructure [D]. Guangzhou: South China University of Technology,2014.
3. Zhang Yuan. Numerical Simulation and Measurement of Local Vibration of Small Coastal Research Ship [D]. Zhoushan: Zhejiang Ocean University,2015.
4. Li Xiu-yan. Research on Vibration Prediction and Local structure Optimization of tuna longline Fishing Vessel [D]. Dalian: Dalian Ocean University,2019.
5. Zhang Qiang. Study on Vibration Reduction of Stern of 1000 ton First Class refined Oil Product Ship [D]. Dalian: Dalian University of Technology, 2017.
6. ZONG Zhi-xiang，WEN Yong-peng. Design method for multiple dynamic absorbers to reduce the vibration of a urban-rail vehicle body [J]. Journal of vibration and shock, 2020,39(02):154-162.
7. ZHANG Ya-xin，LEI Xiao-yan. A model test study on controlling vibration of an elevated track box girder structure with TMD [J]. Journal of vibration and shock, 2021,40(16):220-226+233.
8. TANG Si-cong，WANG Hai-long. Combined optimal design of MTMD system parameter and location applied in reducing floor vibration induced by human-induced loads [J]. Journal of vibration and shock, 2019,38(16):217-223.
9. LIAN Ji-jian，ZHAO Yue. Vibration reduction of offshore wind turbine tube infrastructures based on EC-TMD [J]. Journal of vibration and shock, 2019,38(19):20-25.

 doi:10.20944/preprints202404.1001.v1

10. YANG Ying，JIN Licheng. TMD Vibration reduction analysis and optimal layout for submerged floating tunnel tube under moving load [J].Journal of Vibration and Shock,2024,43(01):165-171.
11. Rahul Rana,Soon T T. Parametric study and simplified design of tuned mass dampers [J]. Engineering Structures, 1998 , 20(3):193-204.
12. LI Bing, LIU Guangshuo. Numerical Simulation of Micro-vibration Response of Steel Structure Workshop under Vehicle Load and TMD Vibration Control [J]. Journal of Shenyang Jianzhu University(Natural Science), 2023, 39 (06): 970-978.
13. CHEN Ling-shuang，LI Shu-jin. Pounding Tuned Mass Damperfor Vibration Control of Barge-type Floating Offshore Wind Turbine Subjected to Combined Wind and Wave Excitations [J]. Journal of Wuhan University of Technology, 2023, 45 (08): 88-94,132.
14. ZHANG Kaidong, TIAN Shizhu. Application of Air Damping Type TMD in Human-induced Vibration Control [J]. Noise and Vibration Control, 2023, 43 (03): 249-253,281.
15. Su Z, Zheng Z, Huang X, et al. Research on dynamic vibration absorber with negative stiffness for controlling longitudinal vibration of propulsion shafting system [J]. Ocean Engineering, 2022, 264: 112375.
16. Ghasemi M R, Shabakhty N, Enferadi M H. Vibration control of offshore jacket platforms through shape memory alloy pounding tuned mass damper (SMA-PTMD) [J]. Ocean Engineering, 2019, 191: 106348.
17. Wu J, Zhu H, Sun Y, et al. Reduction of flexural vibration of a fluid-filled pipe with attached vibration absorbers [J]. International Journal of Pressure Vessels and Piping, 2021, 194: 104525.
18. ZHU da-zhuang,XIONG shi-shu. Study of vibration damping of wind turbine towers by rotary inertia tuned mass dampers [J]. Construction & Design for Engineering,2021,69(23);31-33,36.
19. Bei Hu Yidong. Dynamic Vibration Absorber and Its Application [M]. China Machinery Publishing,2013.
20. LIU Zhen-zhen，JIANG Guo-he. Vibration characteristics of a 100 m new type of polar exploration cruise [J]. Journal of vibration and shock, 2021,40(06):212-219